A New Pseudo Steady-State Constant for a Vertical Well with Finite-Conductivity Fracture

Authors:

Yudong Cui, Bin Lu, Mingtao Wu, Wanjing Luo

Date Submitted: 2018-07-31

Keywords: circular closed reservoir, conductivity-influence function, normalized conductivity-influence function, finite-conductivity fracture, Pseudo Steady-State (PPS) constant

Abstract:

The Pseudo Steady-State (PSS) constant bDpss is defined as the difference between the dimensionless wellbore pressure and dimensionless average pressure of a reservoir with a PSS flow regime. As an important parameter, bDpss has been widely used for decline curve analysis with Type Curves. For a well with a finite-conductivity fracture, bDpss is independent of time and is a function of the penetration ratio of facture and fracture conductivity. In this study, we develop a new semi-analytical solution for bDpss calculations using the PSS function of a circular reservoir. Based on the semi-analytical solution, a new conductivity-influence function (CIF) representing the additional pressure drop caused by the effect of fracture conductivity is presented. A normalized conductivity-influence function (NCIF) is also developed to calculate the CIF. Finally, a new approximate solution is proposed to obtain the bDpss value. This approximate solution is a fast, accurate, and time-saving calculation.

Record Type: Published Article

Submitted To: LAPSE (Living Archive for Process Systems Engineering)

Citation (overall record, always the latest version): LAPSE:2018.0385
Citation (this specific file, latest version): LAPSE:2018.0385-1
Citation (this specific file, this version): LAPSE:2018.0385-1v1

DOI of Published Version: https://doi.org/10.3390/pr6070093

processes

MDPI

Article

A New Pseudo Steady-State Constant for a Vertical Well with Finite-Conductivity Fracture

Yudong Cui [1], Bin Lu [1], Mingtao Wu [2] and Wanjing Luo [1,*]

[1] School of Energy Resources, China University of Geosciences, Beijing 100083, China; CuiYudong1995@126.com (Y.C.); cadbin@163.com (B.L.)
[2] Beijing Key Laboratory of Unconventional Natural Gas Geological Evaluation and Development Engineering, China University of Geosciences, Beijing 100083, China; wumt@cugb.edu.cn
* Correspondence: luowanjing@cugb.edu.cn; Tel.: +86-188-1002-8882

Received: 19 June 2018; Accepted: 9 July 2018; Published: 19 July 2018

Abstract: The Pseudo Steady-State (PSS) constant b_{Dpss} is defined as the difference between the dimensionless wellbore pressure and dimensionless average pressure of a reservoir with a PSS flow regime. As an important parameter, b_{Dpss} has been widely used for decline curve analysis with Type Curves. For a well with a finite-conductivity fracture, b_{Dpss} is independent of time and is a function of the penetration ratio of facture and fracture conductivity. In this study, we develop a new semi-analytical solution for b_{Dpss} calculations using the PSS function of a circular reservoir. Based on the semi-analytical solution, a new conductivity-influence function (CIF) representing the additional pressure drop caused by the effect of fracture conductivity is presented. A normalized conductivity-influence function (NCIF) is also developed to calculate the CIF. Finally, a new approximate solution is proposed to obtain the b_{Dpss} value. This approximate solution is a fast, accurate, and time-saving calculation.

Keywords: Pseudo Steady-State (PPS) constant; finite-conductivity fracture; conductivity-influence function; normalized conductivity-influence function; circular closed reservoir

1. Introduction

Hydraulic fracturing has been widely used to enhance oil and gas recovery [1–9]. Some models have been introduced to describe fluid flow in hydraulic fractures, such as the uniform-flux fracture model [10–12], infinite-conductivity fracture model [10,13,14], and the finite-conductivity fracture model [15–19].

Pseudo steady-state (PSS) is a boundary-dominant flow regime created when pressure waves spread to the boundary in a closed drainage area. In this flow regime, the relationship of dimensionless wellbore pressure and dimensionless average pressure can be expressed as [20–24]:

$$p_{wD} - p_{avgD} = b_{Dpss} \tag{1}$$

where b_{Dpss} is the Pseudo Steady-State (PSS) constant [24]. This PSS constant b_{Dpss} has been widely used to define the appropriate dimensionless decline rate in many currently used production-decline rate analysis models [20,25–28].

When the pressure disturbance reaches to the boundary, the PPS flow regime occurs and the PSS constant b_{Dpss} can be obtained by running a long-term numerical simulation [20,21,23]. Pratikno et al. [20] presented a numerical solution for the PSS constant for a well with a finite-conductivity fracture in a circular closed reservoir (Figure 1).

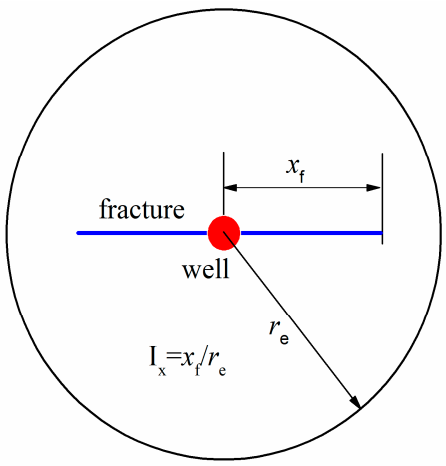

Figure 1. Schematic of a vertical well with a fracture in a circular reservoir.

For convenience, b_{Dpss} is usually approximated as an analytical expression [20,21,23]. Pratikno et al. [20] proposed the following approximate expression:

$$b_{Dpss} = f(r_{eD}) + f\left(C_{fD}\right) \tag{2}$$

where:

$$f(r_{eD}) = \ln(r_{eD}) - 0.049298 + 0.43464/r_{eD}^2 \tag{3}$$

$$f\left(C_{fD}\right) = \frac{0.936268 - 1.00489\psi + 0.319733\psi^2 - 0.0423532\psi^3 + 0.00221799\psi^4}{1 - 0.385539\psi - 0.0698865\psi^2 - 0.0484653\psi^3 - 0.00813558\psi^4} \tag{4}$$

and:

$$\psi = \ln C_{fD} \tag{5}$$

Equation (3) is the pressure drop of a well with an infinite-conductivity fracture in the PSS flow regime [11]. The second term in Equation (2), $f(C_{fD})$, is the additional pressure drop caused by the effect of fracture conductivity. We define $f(C_{fD})$ as the conductivity-influence function (CIF). Thus, the PSS constant b_{Dpss} can be expressed as the sum of the pressure drop of a well with an infinite-conductivity fracture and the conductivity-influence function (CIF). Note that the CIF in Equation (4) is only a function of the fracture conductivity.

Wang et al. [23] also introduced an approximate expression for $f(C_{fD})$ using regression for a circular reservoir.

$$f\left(C_{fD}\right) = \frac{0.95 - 0.56\psi + 0.16\psi^2 + 0.028\psi^3 + 0.0028\psi^4 - 0.00011\psi^5}{1 + 0.094\psi + 0.093\psi^2 + 0.0084\psi^3 + 0.001\psi^4 + 0.00036\psi^5} \tag{6}$$

For the low permeability and ultra-low permeability reservoirs, the elliptical boundary has been used to approximately represent circular a reservoir for calculation of b_{Dpss}. The corresponding conductivity-influence function for an elliptical reservoir was presented by Amini et al. [21]:

$$f\left(C_{fD}\right) = \frac{-4.7468 + 36.2492\psi + 55.0998\psi^2 - 3.98311\psi^3 + 6.07102\psi^4}{-2.4941 + 21.6755\psi + 41.0303\psi^2 - 10.4793\psi^3 + 5.6108\psi^4} \tag{7}$$

In addition, assuming an elliptical boundary, two analytical solutions for a well with an infinite-conductivity fracture and a finite-conductivity fracture were developed by Prats et al. [29] and Lu et al. [24], respectively.

As analyzed from a previous statement, three problems occur with the b_{Dpss} calculation.

(1) The assumption of elliptical flow is an approximate model of the circular boundary [29]. For a fractured well, the real pressure front should be a circle instead of an ellipse during the late-time flow regime.

(2) When C_{fD} trends to infinity, i.e., the infinite-conductivity fracture, Equations (4), (6), and (7) cannot meet the following condition, meaning the limit of conductivity-influence function $f(C_{fD})$ should be zero.

$$\lim_{C_{fD}\to\infty} f\left(C_{fD}\right) = 0 \tag{8}$$

(3) For the existing approximate models [20,21,23], the conductivity-influence function $f(C_{fD})$ is only relative to the fracture conductivity. For different penetration fracture ratios I_x, the distributions in the flow field around the fracture are different, which affects the value of conductivity-influence function (Figure 2). Thus, CIF is not only a function of conductivity, but also related to penetration ratio.

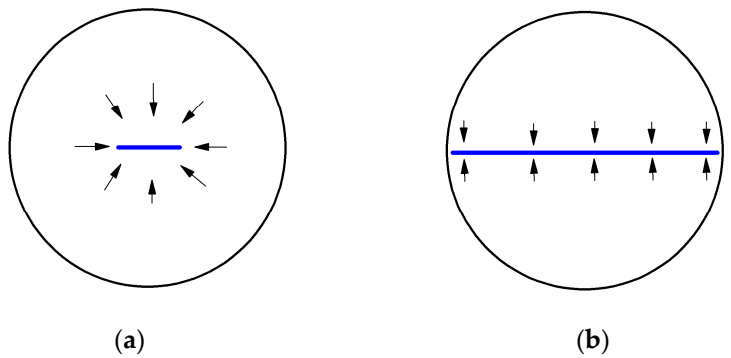

(**a**) (**b**)

Figure 2. Schematic of the flow field around a fracture in a circular reservoir at late-time regime: (**a**) a short fracture with a low penetration ratio and (**b**) a long fracture with high penetration ratio.

In this paper, based on the assumption of a circular closed reservoir, we extended and corrected the work of Pratikno et al. [20]. The contributions of our work include: (1) a semi-analytical method is developed to calculate the b_{Dpss} by use of the PSS function instead of the transient-pressure function [20]; (2) based on the results from the semi-analytical method, a new conductivity-influence function (CIF) is introduced considering the effect of penetration ratio and fracture conductivity has been established; and (3) a new normalized conductivity-influence function (NCIF) is introduced to calculate the value of b_{Dpss}.

2. Mathematical Model

2.1. Basic Assumptions

As shown in Figure 1, a vertical fractured well is located in the center of the circular closed isotropic formation with radius r_e. The flow in the reservoir and fracture is assumed to be single phase and isothermal with a slightly compressible Newtonian fluid. The penetrate ratio I_x is defined as:

$$I_x = \frac{x_f}{r_e} = \frac{1}{r_{eD}} \tag{9}$$

2.2. Semi-Analytical Model for b_{Dpss} Calculation

Different from the transient-pressure-function method presented by Pratikno et al. [20], we derive the semi-analytical model with the PSS function. The advantages of our method include: (1) we can obtain the PSS pressure directly instead of using the long-term approximation of transient pressure, and (2) without the numeric inversion, our method is more accurate and is less time consuming.

2.2.1. Flow Model of the Reservoir

The fracture is equally divided into $2N$ segments. Each segment can be considered as a uniform-flux fracture [30]. Therefore, the uniform-flux solution of a fracture located in a closed circular reservoir can be used to calculate the pressure [11]. To consider the fracture symmetry, we focused on half of the fracture. According to the superposition principle, the dimensionless pressure of the ith segment in the reservoir can be written as:

$$p_{Di} = p_{avgD} + \sum_{j=1}^{2N} q_{Dj} \cdot F_{ij}(x_{Di}, y_{Di}, x_{wDi}, y_{wDi}, r_{eD}), i = 1, 2, 3 \cdots N \tag{10}$$

where F is the function presented by Ozkan [11] for a circular closed reservoir in the PSS flow regime.

Equation (10) can be written in matrix form as:

$$\vec{p}_D - \begin{pmatrix} p_{avgD} \\ p_{avgD} \\ \vdots \\ p_{avgD} \end{pmatrix} = F \cdot \vec{q}_D \tag{11}$$

2.2.2. Flow Model of the Fracture

Luo and Tang [30] derived a wing solution in the discretized form and the pressure of the ith segment, which can be expressed as:

$$P_{wD} - P_{fDi} = \left(\frac{2\pi}{C_{fD}}\right) \cdot \begin{bmatrix} r_{Di} \cdot \sum_{k=1}^{N} q_{fDk} - \left(\frac{\Delta r_{Di}}{8}\right) \cdot q_{fDi} \\ -\sum_{k=1}^{i-1} q_{fDk} \cdot \left[\frac{\Delta r_{Di}}{2} + (r_{Di} - k \cdot \Delta r_{Di})\right] \end{bmatrix}, \mathrm{i} = 1, 2, \ldots \mathrm{N} \tag{12}$$

with

$$r_{Di} = \sum_{k=1}^{i-1} L_{fDk} + L_{fDi}/2, \ \Delta r_{Di} = L_{fDi} \tag{13}$$

Equation (13) can be written in matrix form as:

$$\begin{pmatrix} p_{wD} \\ p_{wD} \\ \vdots \\ p_{wD} \end{pmatrix} - \vec{p}_{fD} = C \cdot \vec{q}_{fD} \tag{14}$$

2.2.3. Semi-Analytical Solution for b_{Dpss}

According to the continuity condition, which states that the pressure and flux must be continuous along the fracture surface, the following conditions must hold along the wing plane:

$$\vec{p_{fD}} = \vec{p_D}, \ \vec{q_{fD}} = \vec{q_D} \tag{15}$$

Substituting Equation (15) into Equations (11) and (14) yields:

$$\begin{pmatrix} p_{wD} \\ p_{wD} \\ \vdots \\ p_{wD} \end{pmatrix} - \begin{pmatrix} p_{avgD} \\ p_{avgD} \\ \vdots \\ p_{avgD} \end{pmatrix} = (C + F) \cdot \vec{q}_{fD} \tag{16}$$

Substituting Equation (1) into Equation (16), we obtain:

$$(C+F)\cdot\vec{q}_{fD}-b_{Dpss}=0 \tag{17}$$

In addition, the total flow rate satisfies the following:

$$\sum_{j=1}^{N} q_{fDi}=\frac{1}{2} \tag{18}$$

b_{Dpss} can be obtained by solving Equations (17) and (18) with the Gauss elimination method.

2.3. Conductivity-Influence Function (CIF)

The procedure to calculate the conductivity-influence function are as follows: (1) Calculate the PSS constant b_{Dpss} for different I_x and C_{fD} using the semi-analytical model in Section 2.2. (2) Calculate the pressure drop of the infinite-conductivity fracture $f(r_{eD})$ for different I_x with Equations (3) and (9). (3) Calculate the difference of b_{Dpss} and $f(r_{eD})$ with Equation (2) and the value of conductivity-influence function (CIF) can be obtained.

Figure 3 presents the CIF for different penetration ratios and fracture conductivities. Different than the solutions obtained by Pratikno et al. [20], the CIF is not only dependent on fracture conductivity but also has a strong relationship with penetration ratio, especially when C_{fD} is less than 10. Additionally, fracture conductivity function tends to be zero when C_{fD} is greater than 300. Table 1 presents the value of the conductivity-influence function for I_x = 0.001–1 and C_{fD} = 0.1–1000.

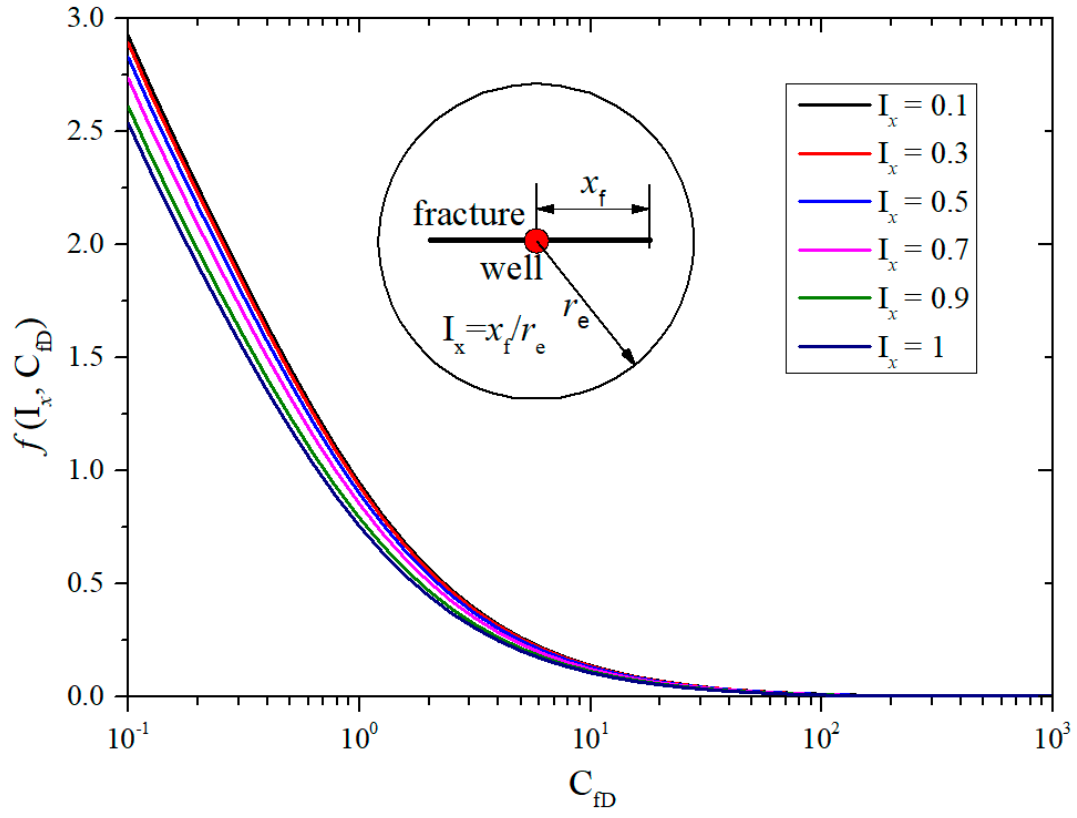

Figure 3. Conductivity-influence function with fracture conductivity (C_{fD}) and penetration ratio (I_x).

Table 1. Conductivity-influence function (CIF) of different penetration ratio (I_x) and fracture conductivity (C_{fD}).

C_{fD}	I_x								
	0.001	**0.05**	**0.01**	**0.05**	**0.1**	**0.3**	**0.5**	**0.8**	**1**
0.1	2.924955	2.923983	2.924917	2.923983	2.921063	2.889918	2.82763	2.675801	2.535652
0.125893	2.694126	2.693183	2.694089	2.693183	2.690353	2.660159	2.599771	2.452575	2.316702
0.158489	2.473614	2.472703	2.473578	2.472703	2.46997	2.440814	2.382503	2.240371	2.109172
0.199526	2.259775	2.258901	2.25974	2.258901	2.256277	2.228293	2.172325	2.035904	1.909976
0.251189	2.050804	2.049971	2.050771	2.049971	2.047474	2.02083	1.967543	1.837656	1.71776
0.316228	1.846441	1.845657	1.84641	1.845657	1.843302	1.818188	1.767959	1.645526	1.532512
0.398107	1.647651	1.64692	1.647622	1.64692	1.644726	1.621328	1.574532	1.460467	1.355176
0.501187	1.456232	1.45556	1.456206	1.45556	1.453543	1.432024	1.388986	1.284082	1.187247
0.630957	1.274395	1.273785	1.274371	1.273785	1.271955	1.252433	1.213389	1.118219	1.03037
0.794328	1.104337	1.103791	1.104315	1.103791	1.102154	1.084688	1.049755	0.964606	0.886007
1	0.9479	0.947418	0.947881	0.947418	0.945973	0.930557	0.899725	0.824572	0.7552
1.258925	0.806339	0.805919	0.806322	0.805919	0.80466	0.791229	0.764366	0.698889	0.638448
1.584893	0.680231	0.67987	0.680217	0.67987	0.678786	0.667223	0.644099	0.587732	0.535701
1.995262	0.569498	0.56919	0.569486	0.56919	0.568267	0.558422	0.538731	0.490735	0.446431
2.511886	0.473515	0.473256	0.473505	0.473256	0.472478	0.464176	0.447573	0.407101	0.369743
3.162278	0.391259	0.391042	0.39125	0.391042	0.390391	0.383452	0.369573	0.335742	0.304514
3.981072	0.321455	0.321276	0.321448	0.321276	0.320736	0.314979	0.303467	0.275404	0.2495
5.011872	0.262718	0.26257	0.262712	0.26257	0.262125	0.257382	0.247898	0.224778	0.203437
6.309573	0.213648	0.213526	0.213643	0.213526	0.213162	0.209279	0.201513	0.182584	0.16511
7.943282	0.17291	0.172811	0.172906	0.172811	0.172514	0.169353	0.16303	0.147618	0.133391
10	0.139273	0.139193	0.13927	0.139193	0.138953	0.136392	0.131272	0.118789	0.107268
12.58925	0.111637	0.111572	0.111634	0.111572	0.111379	0.109316	0.105189	0.095131	0.085847
15.84893	0.089036	0.088984	0.089034	0.088984	0.088829	0.087175	0.083866	0.075802	0.068357
19.95262	0.070637	0.070596	0.070636	0.070596	0.070472	0.069152	0.066513	0.060078	0.054139
25.11886	0.055731	0.055698	0.05573	0.055698	0.0556	0.054552	0.052457	0.047349	0.042633
31.62278	0.043716	0.043691	0.043715	0.043691	0.043613	0.042785	0.04113	0.037096	0.033371
39.81072	0.034091	0.03407	0.03409	0.03407	0.034009	0.033359	0.032058	0.028887	0.02596
50.11872	0.026434	0.026418	0.026433	0.026418	0.02637	0.025861	0.024844	0.022363	0.020074
63.09573	0.020396	0.020383	0.020395	0.020383	0.020346	0.01995	0.019157	0.017225	0.015441
79.43282	0.015687	0.015677	0.015687	0.015677	0.015648	0.015341	0.014725	0.013223	0.011838
100	0.012068	0.012061	0.012068	0.012061	0.012038	0.011799	0.011321	0.010155	0.009078
125.8925	0.009341	0.009335	0.009341	0.009335	0.009318	0.009131	0.008758	0.007849	0.007009
158.4893	0.007342	0.007337	0.007342	0.007337	0.007324	0.007177	0.006883	0.006166	0.005504
199.5262	0.005936	0.005933	0.005936	0.005933	0.005922	0.005803	0.005567	0.004991	0.004459
251.1886	0.005012	0.005009	0.005012	0.005009	0.005	0.004902	0.004706	0.004228	0.003786
316.2278	0.004479	0.004476	0.004478	0.004476	0.004468	0.004383	0.004213	0.003799	0.003417
398.1072	0.004259	0.004257	0.004259	0.004257	0.00425	0.004172	0.004017	0.003639	0.00329
501.1872	0.004292	0.004289	0.004292	0.004289	0.004283	0.004208	0.004059	0.003695	0.003359
630.9573	0.004525	0.004523	0.004525	0.004523	0.004516	0.00444	0.00429	0.003923	0.003584
794.3282	0.004917	0.004914	0.004916	0.004914	0.004907	0.004828	0.00467	0.004285	0.00393
1000	0.005431	0.005429	0.005431	0.005429	0.005421	0.005336	0.005167	0.004753	0.004372

2.4. New Approximate Solution of Pseudo Steady-State Constant b_{Dpss}

Based on the above work, we redefined the PSS constant as the sum of two parts: PSS constant for infinite fracture conductivity [11] and the conductivity-influence function. The PSS constant for infinite fracture conductivity $b_{Dpss,FC}$ is the function of the penetration ratio, and the conductivity-influence function is the function of the penetration ratio and conductivity.

$$b_{Dpss,FC}(I_x, C_{fD}) = b_{Dpss,IC}(I_x) + f(I_x, C_{fD}) \tag{19}$$

where

$$b_{Dpss,IC}(I_x) = -\ln(I_x) - 0.049298 + 0.43464(I_x)^2 \tag{20}$$

We firstly calculate a specific case ($I_x = 0$). As shown in Equation (9):

$$I_x = \lim_{r_e \to \infty} \frac{x_f}{r_e} = \lim_{r_{eD} \to \infty} \frac{1}{r_{eD}} = 0 \tag{21}$$

If the circular closed reservoir is replaced by an infinite-acting reservoir, b_{Dpss} can be approximately replaced by the dimensionless-pressure difference between the finite-conductivity fracture and infinite-conductivity fracture at the radial flow regime for the infinite reservoir [15].

Figure 4 illustrates the CIF of different conductivity at $I_x = 0$ (blue) and $I_x = 1$ (red). Two regression equations for CIF are obtained as follows.

For the case of $I_x = 0$:

$$f_0(C_{fD}) = f(I_x = 0, C_{fD}) = \frac{a_1 u^2 + a_2 u + a_3}{b_1 u^3 + b_2 u^2 + b_3 u + 1} \tag{22}$$

where:

$$u = \ln(C_{fD}) \tag{23}$$

and:

$$\begin{gathered} a_1 = 0.02705;\ a_2 = -0.3123;\ a_3 = 0.9479 \\ b_1 = 0.01736;\ b_2 = 0.1218;\ b_3 = 0.3539 \end{gathered} \tag{24}$$

For the case of $I_x = 1$, the hydraulic fracture fully penetrates the reservoir.

$$f_1(C_{fD}) = f(I_x = 1, C_{fD}) = \frac{a'_1 u^2 + a'_2 u + a'_3}{b'_1 u^3 + b'_2 u^2 + b'_3 u + 1} \tag{25}$$

where:

$$\begin{gathered} a'_1 = 0.02188;\ a'_2 = -0.2509;\ a'_3 = 0.7552 \\ b'_1 = 0.01702;\ b'_2 = 0.1233;\ b'_3 = 0.3798 \end{gathered} \tag{26}$$

We notice that in our model, Equations (22) and (25) meet the following condition:

$$\lim_{C_{fD} \to \infty} f_0(C_{fD}) = \lim_{C_{fD} \to \infty} f_1(C_{fD}) = 0 \tag{27}$$

Moreover, we define a normalized fracture conductivity function (NCIF) as follows:

$$\hat{f}(I_x, C_{fD}) = \frac{f(I_x, C_{fD}) - f_0(C_{fD})}{f_1(C_{fD}) - f_0(C_{fD})} \tag{28}$$

We calculate the CIF for I_x = 0.001–1 and C_{fD} = 0.1–1000 with the method in Sections 2.2 and 2.3. Ten values were calculated for each logarithmic period. Thus, 1200 values of CIF were obtained. The values of NCIF can be calculated using Equation (28).

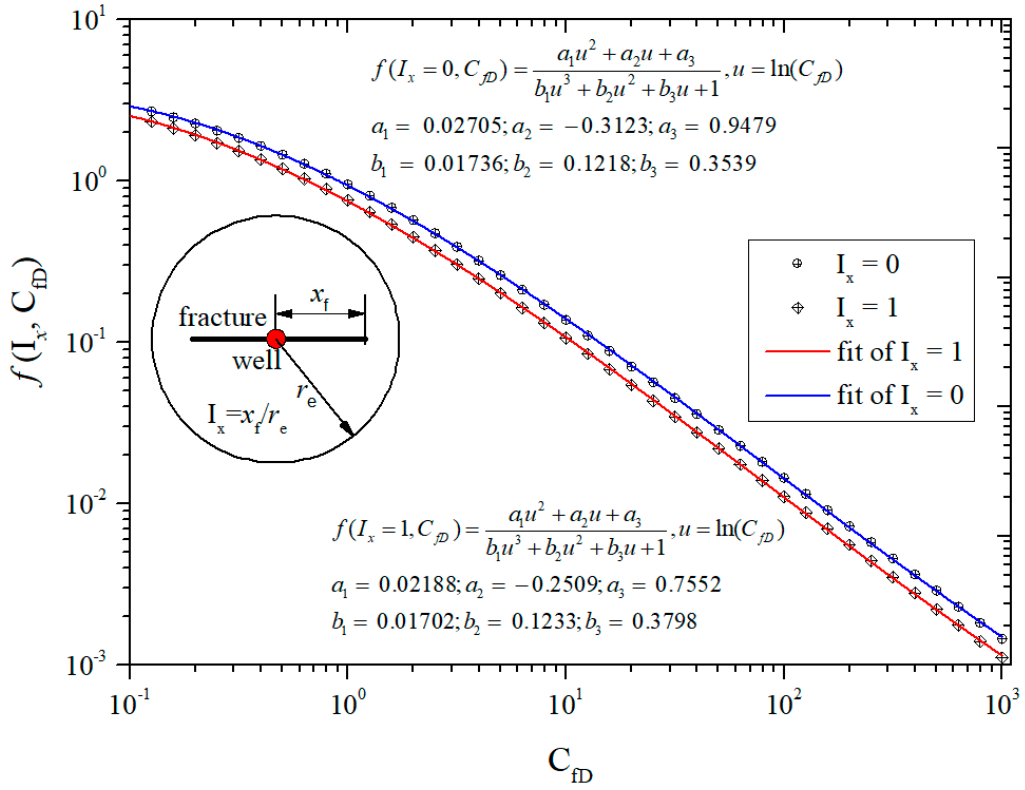

Figure 4. Regression of conductivity-influence function when the penetration ratio (I_x) equals 0 and 1.

Figure 5 shows the relationship between NCIF and I_x. Notably, all data fall in the same straight line in logarithmic coordinates. This means that the NCIF is solely dependent on penetration ratio I_x.

A regression equation can be obtained for NCIF.

$$\hat{f}(I_x, C_{fD}) = \frac{f(I_x, C_{fD}) - f_0(C_{fD})}{f_1(C_{fD}) - f_0(C_{fD})} = I_x^{2.00592} \approx I_x^2 \tag{29}$$

Note that if I_x = 0, the NCIF is equal to 0 in Equation (29).

Recasting Equation (29) yields:

$$f(I_x, C_{fD}) = I_x^2[f_1(C_{fD}) - f_0(C_{fD})] + f_0(C_{fD}) \tag{30}$$

The limit of Equation (30) is equal to zero.

$$\lim_{C_{fD}\to\infty} f(I_x, C_{fD}) = 0 \tag{31}$$

Substituting Equations (20) and (30) into Equation (19), we obtain:

$$b_{Dpss,FC}(I_x, C_{fD}) = \underbrace{-\ln(I_x) - 0.049298 + 0.43464(I_x)^2}_{b_{Dpss,IC}(I_x)} + \underbrace{I_x^2[f_1(C_{fD}) - f_0(C_{fD})] + f_0(C_{fD})}_{f(I_x, C_{fD})} \tag{32}$$

Based on our work, a new b_{Dpss} is presented in Equation (32).

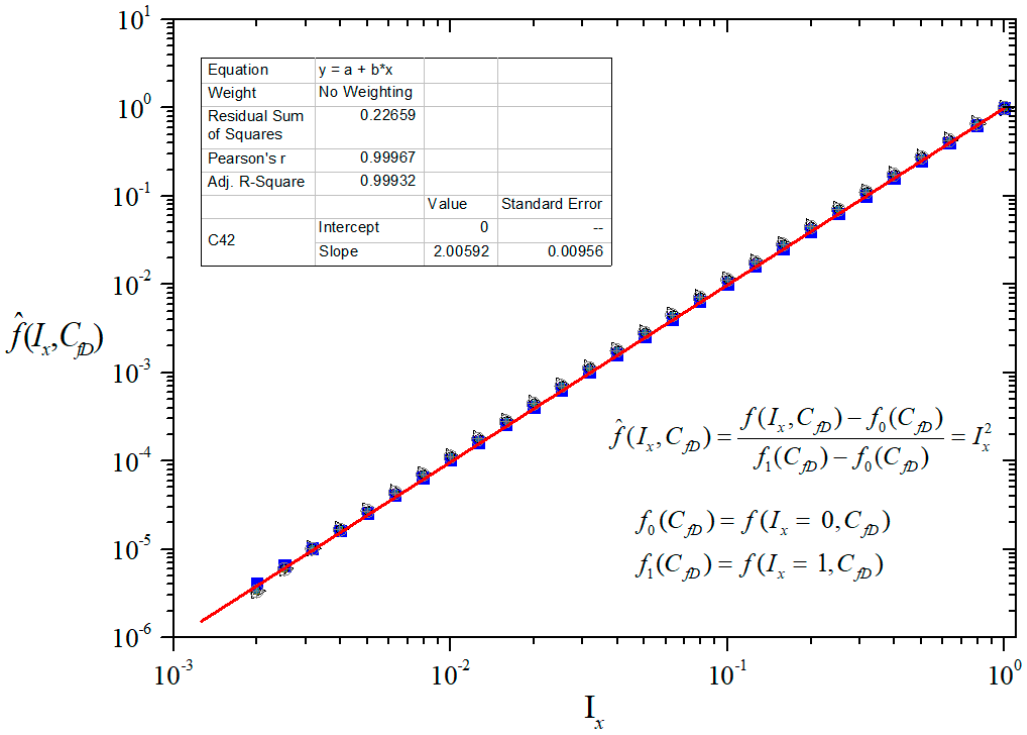

Figure 5. Regression of normalized conductivity-influence function (1200 data points).

3. Results

In this section, we will compare our approximate model with our semi-analytical model and Pratikno et al.'s approximate solutions [20] for different penetrate ratio and fracture conductivity. Table 2 presents the values of b_{Dpss} obtained by our semi-analytical method, Pratikno et al.'s method and our approximate model. As shown in Table 2, the maximum relative error is 0.4% at I_x = 0.1 and 1.93% at I_x = 1 between our approximate model and semi-analytical model. However, huge differences between Pratikno et al.'s method and our semi-analytical method can be observed at large penetration ratio, for example, relative error 16.57% at C_{fD} = 0.631 and I_x = 1.

We further show the comparisons in Figure 6. The circles with crosses, red lines, and blue lines correspond to the semi-analytical solutions (accurate solutions), Pratikno et al.'s solutions, and approximate solutions, respectively. As shown in Figure 6, an excellent agreement among the three methods is visible when the dimensionless fracture conductivity C_{fD} is greater than 10 for all penetration ratios. The lines cross the centers of circles at low penetration ratios, such as I_x values less than 0.3. For these cases, the differences among the three models can be ignored. Our approximate solutions (blue lines) match very well with semi-analytical solutions (circles with cross) for all penetration ratios and fracture conductivities. The red lines deviate from the circles and blue lines and huge differences between Pratikno et al.'s solutions and our solutions are noticeable at low conductivity (C_{fD} < 10) with a high penetration ratio (I_x > 0.5).

Table 2. Comparisons of b_{Dpss} for different calculation methods.

	Semi-Analytical Solutions (This Study)			H.Pratikno et al. Solutions (2003) SPE 84287			Approximate Solutions (This Study)			Relative Error between H.Pratikno et al. Solutions and Semi-Analytical Solutions, %			Relative Error between Semi-Analytical Solutions and Approximate Solutions, %		
C_{fD}	Ix = 0.1	Ix = 0.5	Ix = 1	Ix = 0.1	Ix = 0.5	Ix = 1	Ix = 0.1	Ix = 0.5	Ix = 1	Ix = 0.1	Ix = 0.5	Ix = 1	Ix = 0.1	Ix = 0.5	Ix = 1
0.1000	5.1692	3.5727	2.9135	5.1960	3.6909	3.3237	5.1787	3.5801	2.9210	0.52	3.31	14.08	0.18	0.21	0.26
0.1259	4.9454	3.3517	2.7003	4.9595	3.4544	3.0872	4.9480	3.3523	2.7020	0.29	3.06	14.33	0.05	0.02	0.06
0.1585	4.7252	3.1350	2.4928	4.7319	3.2268	2.8596	4.7276	3.1350	2.4945	0.14	2.93	14.72	0.05	0.00	0.07
0.1995	4.5091	2.9230	2.2915	4.5115	3.0064	2.6392	4.5139	2.9248	2.2953	0.05	2.85	15.18	0.11	0.06	0.17
0.2512	4.2979	2.7163	2.0972	4.2976	2.7924	2.4253	4.3051	2.7201	2.1031	0.01	2.80	15.64	0.17	0.14	0.28
0.3162	4.0924	2.5160	1.9111	4.0902	2.5850	2.2179	4.1009	2.5205	1.9179	0.05	2.74	16.05	0.21	0.18	0.35
0.3981	3.8940	2.3234	1.7340	3.8902	2.3851	2.0179	3.9024	2.3270	1.7405	0.10	2.66	16.37	0.22	0.16	0.37
0.5012	3.7040	2.1396	1.5672	3.6989	2.1938	1.8267	3.7112	2.1415	1.5726	0.14	2.53	16.55	0.19	0.09	0.34
0.6310	3.5242	1.9663	1.4118	3.5181	2.0130	1.6458	3.5296	1.9659	1.4157	0.17	2.37	16.57	0.15	0.02	0.27
0.7943	3.3560	1.8048	1.2687	3.3493	1.8442	1.4770	3.3598	1.8023	1.2713	0.20	2.18	16.42	0.11	0.14	0.21
1.0000	3.2008	1.6563	1.1386	3.1939	1.6888	1.3216	3.2036	1.6522	1.1405	0.21	1.96	16.08	0.09	0.25	0.17
1.2589	3.0597	1.5217	1.0218	3.0530	1.5479	1.1807	3.0623	1.5169	1.0238	0.22	1.72	15.55	0.09	0.32	0.19
1.5849	2.9333	1.4015	0.9186	2.9271	1.4220	1.0548	2.9364	1.3966	0.9210	0.21	1.46	14.83	0.10	0.35	0.27
1.9953	2.8219	1.2957	0.8285	2.8162	1.3111	0.9439	2.8259	1.2912	0.8318	0.20	1.18	13.94	0.14	0.35	0.40
2.5119	2.7249	1.2039	0.7508	2.7198	1.2147	0.8475	2.7301	1.2001	0.7551	0.19	0.89	12.89	0.19	0.32	0.57
3.1623	2.6418	1.1253	0.6847	2.6371	1.1320	0.7648	2.6480	1.1221	0.6899	0.18	0.60	11.71	0.24	0.29	0.75
3.9811	2.5713	1.0587	0.6290	2.5671	1.0620	0.6948	2.5784	1.0560	0.6348	0.16	0.31	10.47	0.28	0.26	0.93
5.0119	2.5121	1.0030	0.5825	2.5068	1.0017	0.6345	2.5198	1.0004	0.5888	0.21	0.12	8.93	0.30	0.26	1.06
6.3096	2.4630	0.9567	0.5441	2.4585	0.9534	0.5862	2.4708	0.9540	0.5505	0.18	0.35	7.73	0.31	0.28	1.15
7.9433	2.4225	0.9186	0.5126	2.4180	0.9129	0.5457	2.4301	0.9155	0.5187	0.19	0.62	6.46	0.31	0.33	1.19
10.0000	2.3894	0.8874	0.4868	2.3847	0.8796	0.5124	2.3966	0.8838	0.4926	0.20	0.88	5.26	0.30	0.41	1.18
12.5893	2.3625	0.8620	0.4659	2.3576	0.8525	0.4853	2.3690	0.8577	0.4712	0.20	1.11	4.17	0.28	0.51	1.12
15.8489	2.3406	0.8415	0.4490	2.3356	0.8305	0.4633	2.3465	0.8364	0.4537	0.21	1.31	3.19	0.25	0.61	1.04
19.9526	2.3230	0.8249	0.4354	2.3179	0.8128	0.4456	2.3281	0.8190	0.4395	0.22	1.47	2.35	0.22	0.72	0.93
25.1189	2.3088	0.8116	0.4244	2.3037	0.7985	0.4314	2.3132	0.8050	0.4280	0.22	1.61	1.64	0.19	0.83	0.83
31.6228	2.2974	0.8009	0.4157	2.2923	0.7872	0.4200	2.3012	0.7936	0.4187	0.22	1.72	1.04	0.17	0.92	0.73
39.8107	2.2883	0.7924	0.4086	2.2832	0.7781	0.4109	2.2916	0.7846	0.4113	0.22	1.80	0.56	0.15	0.99	0.65
50.1187	2.2810	0.7855	0.4030	2.2760	0.7709	0.4037	2.2840	0.7774	0.4054	0.22	1.86	0.18	0.13	1.05	0.59
63.0957	2.2752	0.7801	0.3986	2.2703	0.7652	0.3980	2.2780	0.7717	0.4008	0.21	1.90	0.13	0.12	1.09	0.56
79.4328	2.2705	0.7757	0.3950	2.2658	0.7607	0.3935	2.2733	0.7672	0.3972	0.21	1.93	0.36	0.12	1.10	0.55
100.0000	2.2668	0.7722	0.3921	2.2623	0.7572	0.3900	2.2697	0.7638	0.3944	0.20	1.95	0.55	0.12	1.10	0.58
125.8925	2.2639	0.7695	0.3899	2.2595	0.7543	0.3872	2.2670	0.7613	0.3924	0.20	1.96	0.69	0.13	1.08	0.63
158.4893	2.2616	0.7673	0.3881	2.2573	0.7521	0.3850	2.2650	0.7594	0.3908	0.19	1.97	0.80	0.15	1.04	0.71
199.5262	2.2597	0.7655	0.3866	2.2555	0.7504	0.3832	2.2636	0.7581	0.3898	0.19	1.98	0.89	0.17	0.98	0.81

Table 2. *Cont.*

	Semi-Analytical Solutions (This Study)			H.Pratikno et al. Solutions (2003) SPE 84287			Approximate Solutions (This Study)			Relative Error between H.Pratikno et al. Solutions and Semi-Analytical Solutions, %			Relative Error between Semi-Analytical Solutions and Approximate Solutions, %		
251.1886	2.2582	0.7641	0.3855	2.2541	0.7489	0.3818	2.2626	0.7572	0.3891	0.18	1.99	0.97	0.20	0.91	0.93
316.2278	2.2570	0.7630	0.3846	2.2529	0.7478	0.3806	2.2621	0.7567	0.3888	0.18	2.00	1.04	0.22	0.83	1.07
398.1072	2.2561	0.7621	0.3839	2.2519	0.7468	0.3796	2.2619	0.7565	0.3886	0.19	2.01	1.11	0.26	0.74	1.23
501.1872	2.2553	0.7614	0.3833	2.2511	0.7459	0.3788	2.2619	0.7566	0.3887	0.19	2.03	1.18	0.29	0.64	1.39
630.9573	2.2547	0.7609	0.3828	2.2503	0.7452	0.3780	2.2621	0.7568	0.3889	0.20	2.06	1.26	0.33	0.54	1.56
794.3282	2.2543	0.7604	0.3825	2.2496	0.7445	0.3774	2.2625	0.7572	0.3893	0.21	2.09	1.34	0.37	0.43	1.74
1000	2.2539	0.7601	0.3822	2.2490	0.7439	0.3767	2.2631	0.7577	0.3897	0.22	2.13	1.44	0.40	0.32	1.93

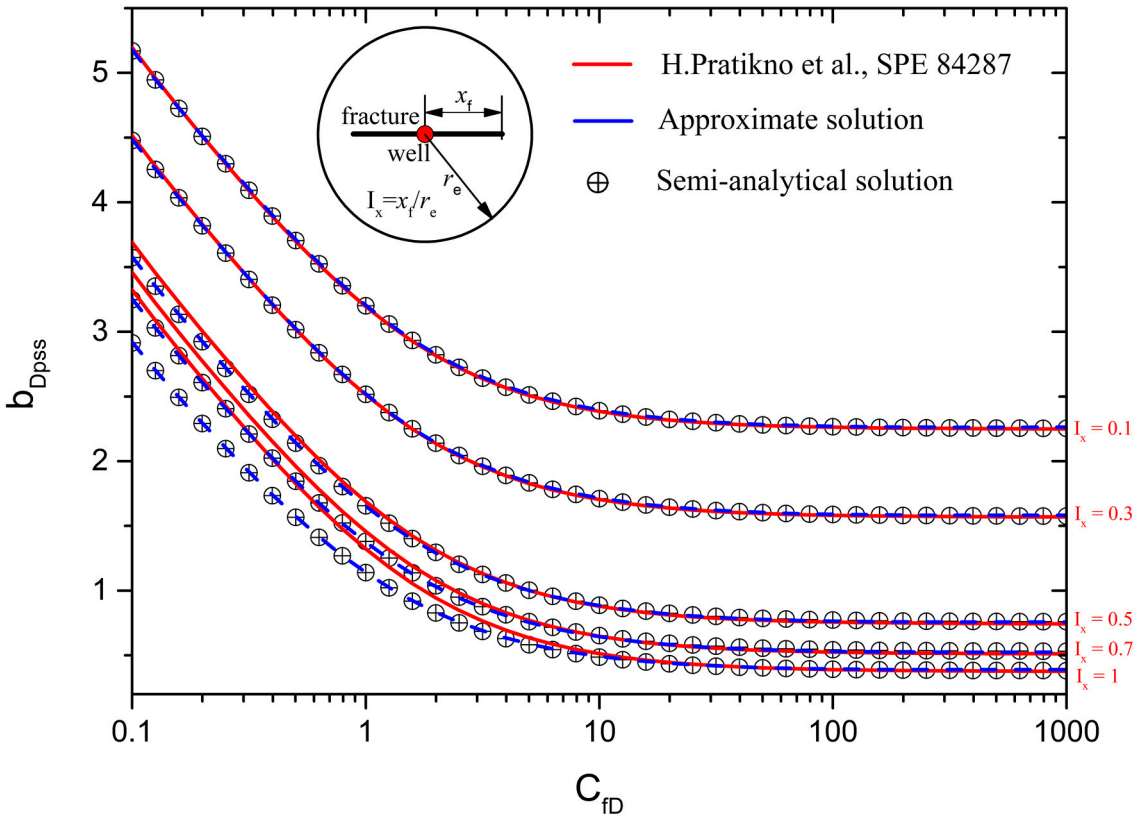

Figure 6. Comparisons of b_{Dpss} with our solutions and Pratikno et al.'s solutions.

4. Conclusions

The following conclusions can be drawn from this study: (1) Pratikno et al. [20] stated that only the fracture conductivity affected the conductivity-influence function (CIF) described in Equation (4). Based on our work, we found that both the fracture conductivity and penetration ratio exerted significant influences on CIF. As Figure 3 shows, CIF decreases with increasing fracture conductivity, and CIF tends to be zero when C_{fD} is greater than 300. Additionally, CIF has obviously differences, especially when C_{fD} is less than 10; the CIF decreases with increasing penetration ratio. (2) Based on the PSS function [11], a new semi-analytical model was proposed to directly calculate the b_{Dpss}, which consumes less time. Besides, our method is more accurate due to simultaneously considering both fracture conductivity and penetration ratio. (3) A new conductivity-influence function (CIF), considering the effect of penetration ratio and fracture conductivity, was developed. A normalized conductivity-influence function (NCIF) was also developed to calculate the value of CIF. Our work provides a fast, accurate, and time-saving method to evaluate b_{Dpss} for a well with a finite-conductivity fracture in a circular closed reservoir.

Author Contributions: Conceptualization, W.L.; Data curation, Y.C., B.L. and M.W.; Formal analysis, B.L.; Investigation, Y.C.; Methodology, W.L.; Project administration, W.L.; Software, Y.C. and M.W.; Supervision, W.L.; Validation, M.W.; Writing—original draft, Y.C.

Funding: This research was funded by [National Natural Science Foundation of China] grant number [51674227].

Acknowledgments: This work was supported by the National Natural Science Foundation of China (Grant No. 51674227) and the Fundamental Research Funds for the Central Universities.

Conflicts of Interest: The authors declare no conflict of interest.

References

1. Wasantha, P.L.P.; Konietzky, H. Fault reactivation and reservoir modification during hydraulic stimulation of naturally-fractured reservoirs. *J. Nat. Gas Sci. Eng.* **2016**, *34*, 908–916. [CrossRef]
2. Ghaderi, S.M.; Clarkson, C.R. Estimation of fracture height growth in layered tight/shale gas reservoirs using flowback gas rates and compositions—Part I: Model development. *J. Nat. Gas Sci. Eng.* **2016**, *36*, 1018–1030. [CrossRef]
3. Taheri-Shakib, J.; Ghaderi, A.; Hosseini, S.; Hashemi, A. Debonding and coalescence in the interaction between hydraulic and natural fracture: Accounting for the effect of leak-off. *J. Nat. Gas Sci. Eng.* **2016**, *36*, 454–462. [CrossRef]
4. Li, B.; Liu, R.; Jiang, Y. Influences of hydraulic gradient, surface roughness, intersecting angle, and scale effect on nonlinear flow behavior at single fracture intersections. *J. Hydrol.* **2016**, *538*, 440–453. [CrossRef]
5. Liu, R.; Li, B.; Jiang, Y. A fractal model based on a new governing equation of fluid flow in fractures for characterizing hydraulic properties of rock fracture networks. *Comput. Geotech.* **2016**, *75*, 57–68. [CrossRef]
6. Liu, R.; Li, B.; Jiang, Y. Critical hydraulic gradient for nonlinear flow through rock fracture networks: The roles of aperture, surface roughness, and number of intersections. *Adv. Water Res.* **2016**, *88*, 53–65. [CrossRef]
7. Haeri, F.; Izadi, M.; Zeidouni, M. Unconventional multi-fractured analytical solution using dual porosity model. *J. Nat. Gas Sci. Eng.* **2017**, *45*, 230–242. [CrossRef]
8. Al-Rbeawi, S. Analysis of pressure behaviors and flow regimes of naturally and hydraulically fractured unconventional gas reservoirs using multi-linear flow regimes approach. *J. Nat. Gas Sci. Eng.* **2017**, *45*, 637–658. [CrossRef]
9. Oyedokun, O.; Schubert, J. A quick and energy consistent analytical method for predicting hydraulic fracture propagation through heterogeneous layered media and formations with natural fractures: The use of an effective fracture toughness. *J. Nat. Gas Sci. Eng.* **2017**, *44*, 351–364. [CrossRef]
10. Gringarten, A.C.; Ramsey, H.J., Jr.; Raghavan, R. Unsteady Pressure Distribution Created by a Well with a Single Infinite-Conductivity Vertical Fracture. *SPE J.* **1974**, *14*, 347–360. [CrossRef]
11. Ozkan, E. Performance of Horizontal Wells. Ph.D. Thesis, University of Tulsa, Tulsa, OK, USA, 1988.
12. Ozkan, E.; Raghavan, R. Some new solutions to solve problems in well test analysis: I. Computational considerations and applications. *SPE Form. Eval.* **1991**, *6*, 359–368. [CrossRef]
13. Kuchuk, F.J.; Goode, P.A.; Wilkinson, D.J.; Thambynayagam, R.K.M. Pressure-transient behavior of horizontal wells with and without gas cap or aquifer. *SPE Form. Eval.* **1991**, *6*, 86–94. [CrossRef]
14. Hagoort, J. The productivity of a well with a vertical infinite-conductivity fracture in a rectangular closed reservoir. *SPE J.* **2009**, *14*, 715–720. [CrossRef]
15. Cinco-Ley, H.; Samaniego, V.F.; Dominguez, A.N. Transient Pressure Behavior for a Well with a Finite-Conductivity Vertical Fracture. *SPE J.* **1978**, *18*, 253–264. [CrossRef]
16. Cinco-Ley, H.; Meng, H.Z. Pressure transient of wells with finite conductivity vertical fractures in double porosity reservoirs. Presented at the SPE Annual Technical Conference and Exhibition, Houston, TX, USA, 2–5 October 1988.
17. Lee, S.T.; Brockenbrouth, J.R. A new approximate analytic solution for finite conductivity vertical fractures. Presented at the SPE annual technical conference and exhibition, San Francisco, CA, USA, 5–8 October 1986.
18. Blasingame, T.A.; Poe, B.D. Semianalytic solutions for a well with a single finite-conductivity vertical fracture. Presesnted at the SPE Annual Technical Conference and Exhibition, Houston, TX, USA, 3–6 October 1993.
19. Luo, W.; Tang, C. A semi-analytical solution of a vertical fractured well with varying conductivity under non-darcy-flow condition. *SPE J.* **2015**, *20*, 1028–1040. [CrossRef]
20. Pratikno, H.; Rushing, J.A.; Blasingame, T.A. Decline Curve Analysis Using Type Curves—Fractured Wells. In Proceedings of the SPE Annual Technical Conference and Exhibition. Society of Petroleum Engineers, Denver, Colorado, 5–8 October 2003.
21. Amini, S.; Liik, D.; Blasingame, T.A. Evaluation of the Elliptical Flow Period for Hydraulically-Fracture Wells in Tight Gas Sands-Theoretical Aspects and Practical Considerations. Presented at the SPE Hydraulic Fracturing Technology Conference, College Station, TX, USA, 29–31 January 2007.
22. Hagoort, J. Semisteady-State Productivity of a Well in a Rectangular Reservoir Producing at Constant Rate or Constant Pressure. *SPE Res. Eval. Eng.* **2011**, *14*, 677–686. [CrossRef]

23. Wang, L.; Wang, X.D.; Ding, X.M.; Chen, L. Rate Decline Curves Analysis of a Vertical Fractured Well with Fracture Face Damage. *J. Energy Resour. Technol.* **2012**, *134*, 032803. [CrossRef]
24. Lu, Y.; Chen, K.P. Productivity-Index Optimization for Hydraulically Fractured Vertical Wells in a Circular Reservoir: A Comparative Study with Analytical Solutions. *SPE J.* **2016**, *21*, 2208–2219. [CrossRef]
25. Fetkovich, M.J. Decline Curve Analysis Using Type Curves. *J. Pet. Technol.* **1980**, *32*, 1065–1077. [CrossRef]
26. Fetkovich, M.J.; Vienot, M.E.; Bradley, M.D.; Kiesow, U.G. Decline Curve Analysis Using Type Curves—Case Histories. *SPE Form. Eval.* **1987**, *2*, 637–656. [CrossRef]
27. Doublet, L.E.; Blasingame, T.A. Decline Curve Analysis Using Type Curves: Water Influx/Waterflood Cases. Presented at the 1995 Annual SPE Technical Conference and Exhibition, Dallas, TX, USA, 22–25 October 1995.
28. Agarwal, R.G.; Gardner, D.C.; Kleinsteiber, S.W.; Fussell, D.D. Analyzing Well Production Data Using Combined-Type-Curve and Decline-Curve Analysis Concepts. In Proceedings of the SPE Annual Technical Conference and Exhibition, Society of Petroleum Engineers, Houston, TX, USA, 3–6 October 1999; pp. 478–486.
29. Prats, M.; Hazebroek, P.; Strickler, W.R. Effect of vertical fractures on reservoir behavior–compressible-fluid case. *SPE J.* **1962**, *2*, 87–94. [CrossRef]
30. Luo, W.; Wang, X.; Tang, C.; Feng, Y.; Shi, E. Productivity of multiple fractures in a closed rectangular reservoir. *J. Pet. Sci. Eng.* **2017**, *157*, 232–247. [CrossRef]